Investigation of the hippocampal information processing in freely moving rats

Summary of the Ph.D. thesis

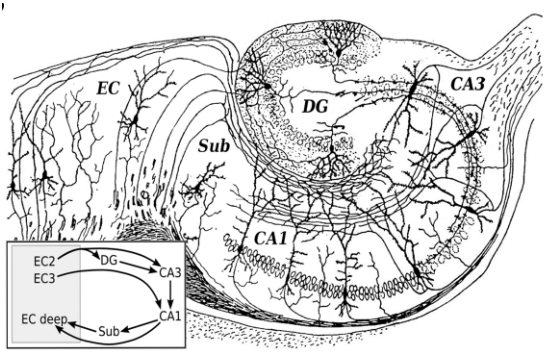

Azahara Oliva

University of Szeged, Department of Physiology

Szeged

2016

Introduction

A major goal of neuroscience is to understand how the brain generates complex behaviors. The present work focuses on the information processing of the hippocampus (HP) in behaving rats, an important region for high cognitive functions.

Anatomically, the HP is divided in four regions: CA1, CA2, CA3 and dentate gyrus (DG). CA1 is further split into proximal, middle, and distal subregions, while CA3 is divided into CA3a (close to CA2), b, and c (close to DG) parts. Along these divisions, the cells are organized in parallel, compact, and uniform layers. The strongest input to the HP is the entorhinal cortex (EC) through the "trisynaptic circuit", which includes the "perforant pathway" from the EC layer II (LII) to the DG, the "mossy fiber" projection to the CA3 region and the "Schaffer collaterals" from CA3 to CA1. The CA1 sends the information back to the subiculum and the deep layers (layer V-LV) of the EC, and from there to other areas. Some parallel routes go from LII (EC) to CA3 and CA2 regions and from layer III (LIII) to CA1. Also, the distinct parts of EC project preferentially to distinct parts of CA1: the medial entorhinal cortex (MEC) mainly target the proximal pole and the lateral entorhinal cortex (LEC) the distal one.

The firing patterns in vivo are mainly shaped by the synaptic inputs and the intrinsic properties of the cells. Pyramidal cells in the HP fire slow [0.5-2 Hz] and occasionally in bursts. Interneurons fire faster, in a broad range [2-3 Hz to 10-30 Hz]. The distinct features of action potentials

recorded in the extracellular signals correlate with the distinct types of neurons, allowing the classification of the neurons from the extracellular signals.

The single cell activity of the HP is characterized by the responses of the principal cells to the position of the animal. Cells, which become active (increase their firing rate – FR) when the animal enters a particular location in the environment (and are inactive when the animal is out) are called “place cells”. The location in which the cell remains active is called “place field” and each place cell can have from one to several such fields.

The population activity patterns of the HP are easy to recognize due to the very characteristic field potentials (LFP). One of the most prominent patterns is the theta oscillation (present during locomotion, exploration and rapid eyes movement (REM) sleep). This wave of 5-10 Hz entrains nearly all neurons in the HP, and each region (CA1, CA2, CA3) becomes active in different phases of the cycle. The mechanisms of theta generation are still unknown, with a consensus about the septum as the main pacer of this oscillation. One interesting phenomenon regarding theta rhythm is the advance toward earlier phases of the spikes of place cells inside their place fields, known as phase precession.

Another distinctive pattern is the sharp wave-ripple (SPW-R). SPW-Rs consist of a negative and slow deflection in the stratum radiatum (sharp wave, SPW) and a fast oscillation (~140 Hz) in the pyramidal layer (ripple). The CA3a subregion is known to be implicated in the generation

of SPW, specifically through the activity of CA3a pyramidal cells and their extensive recurrent collaterals, which contribute to the generation of population events. The CA2 region mirrors some aspects of CA3a, however, its contribution to SPW-Rs has been traditionally neglected. SPW-Rs patterns are involved in the consolidation of recent memories during immobility and non-REM sleep.

Another patterns of the HP are the gamma oscillations, which are defined as 30-150 Hz oscillations and are related to attention and sensory processing. They can be observed in different layers with different frequencies respectively. Although initially gamma oscillations were considered a unitary phenomenon, evidence suggests that there are several mechanisms account for these patterns.

The functional role of the HP has been extensively studied since the discovery of its importance in memory and spatial navigation. A famous human study involving the surgical removal of the HP resulted in an impairment of the ability of the subject to form new memories. Since then, neurophysiological and anatomical studies helped to conclude that the HP is crucial for episodic memory. The other main function of the HP was discovered when pyramidal cells (place cells) of the CA1 region of rats were found to fire at particular spatial locations. As a synthesis, HP was proposed to be the locus of “a spatial and a cognitive map”. Since then, many studies have clarified how the different regions of the HP contribute to the generation and dynamic update of these “maps”.

Aims of the study

The aims of this study were to examine the information processing in the HP of freely moving rats from all subregions simultaneously. We provide electrophysiological data about the differences within the various neuron populations of the HP. Our specific aims were:

- To investigate the physiological differences within CA1, CA2 and CA3 regions at the cellular level during behavior.
- To characterize the spatio-temporal dynamics of the network during the information flow between HP regions.
- To investigate the specialization of the different subregions of the CA1, CA2 and CA3 during spatial coding.
- To examine the relationship between synaptic inputs and local network activity in each subregion of the HP.

Materials and Methods

Long-Evans rats were operated under isoflurane anesthesia. A craniotomy was performed with stereotaxic guidance and a silicon probe was implanted covering CA1, CA2 and CA3 regions simultaneously. A movable microdrive was attached to the skull with dental cement and a screw allowed advancing the probe every day. A cooper mesh was attached to the skull and connected to the ground to avoid noise. The electrode was connected to a multiplexing headstage attached to a cable, which allowed free movement of the animal. Two LEDs were attached to the cooper mesh to track the position. Neuronal activity was recorded

during sleep, running in a linear track, and memory tasks performance in various mazes. The signal was acquired at 20kSamples/s (KJE-1001, Amplipex Ltd, Hungary). LFP signal was generated (down sampling the signal to 1250 Hz) and neuronal spikes were detected using a high-pass filter (0.5-5 kHz) in spikedetekt2 software. Spikes were automatically clustered with Klustawik2 software and manually adjusted with KlustaViewa software.

After terminating the experiments, animals were perfused with 0.9% saline solution followed by 4% paraformaldehyde. Brains were sliced (70um thickness in Leica Vibratome) and immunolabelled with PCP4 (specific CA2 marker). For this, slices were washed three times in PBS-Tx 1%, blocked with 3% bovine serum albumin in PBX-Tx 1% and incubated overnight with the primary antibody solution (rabbit anti-PCP4 -1:300). Finally, slices were washed three times in PBX-Tx and incubated for 2h with goat anti-rabbit Alexa Fluor-488 (1:500). Slices were mounted in glass slides with fluorescence medium.

All analyses were made in MATLAB, using toolboxes and custom-made routines. The position of the animal was recorded and the rate maps were obtained as the spike count map divided by the time spent in 5 cm bins. A place field was defined as a contiguous region of at least 15 cm, with a FR higher than 10% of the peak rate in the maze. The number of place fields, spatial information and selectivity were calculated for each cell. For each place field, the instantaneous phase of each spike was calculated. We plotted the phase of spikes inside the theta cycle against the position to visualize phase precession. A circular-linear regression

was calculated for the position versus theta phase and the slope, strength and phase range of the spikes were computed.

To evaluate theta epochs, we band-pass filtered the CA1 pyramidal layer LFP in the theta frequency (5-11 Hz). Theta epochs during running were labeled as RUN and during sleep as REM. Low theta power and low speed periods (less than 2 cm/s) periods during wakefulness or sleep were classified as WAKE or as non-REM sleep, respectively. Theta phase was obtained from the Hilbert transform, with peaks selected as 0° and troughs as 180°. The theta modulation index was calculated using the mean resultant length of the spike phases and Rayleigh test was used to consider significance. To study the spike-theta phase relationship we used the distribution of all spikes phases and the distribution of the preferred phases of all significant modulated cells.

To detect ripples we excluded theta epochs and filtered the LFP of the pyramidal layers in the frequency of interest (80-250 Hz). A four standard deviation (SD) threshold was applied to the signal power to detect ripple events, which were expanded until the power fell below two SDs. The closest trough to the peak was used to align all events (considered as the “0” time). This process was computed on a single reference channel of every shank independently.

To analyze the neuronal firing during ripples we considered ripples from different regions (CA1, CA2 and CA3) independently. The duration of each ripple was normalized for every recording session. For each individual neuron, we considered all spikes around the ripples (100 ms window). We built ripple cross-correlograms and set the 95% confidence

interval to classify the neuron as positively or negatively modulated by ripples. For every cell, we constructed a peri-ripple (100 ms window) FR histogram. For the population average, we used the z-scored values of the FR histograms.

To study the peri-ripple activity of the different regions (CA1, CA2 and CA3 population), we calculated CCGs with the spikes of the cells from these regions in a peri-ripple window and compared all pairs of neurons between the two regions. For each CCG, spikes of the spike train were randomly jittered (50 ms interval) to build a surrogate data set and detect significant time bins of spike transmission between regions. Also, CCGs between pair of neurons were calculated to look for functional monosynaptic connections. CCGs with significant peaks within 5 ms were considered as a signature for monosynaptically connected pairs.

Results

Animals were recorded from all regions of the HP simultaneously and LFPs and units activity from all layers were recorded. Different regions and subregions were separated based on physiological criteria, difference in the width of the pyramidal layer and validated with immunohistology.

State-dependent firing patterns and functional connectivity across regions

We examined the FR of the neurons to study the functional differences between subpopulations during the distinct behavioral states. FRs of CA2 cells were the highest for all brain states, followed by CA1 and CA3 neurons. CA1 proximal cells had higher FRs than distal ones while CA3

distal (CA3a) cells fired more than proximal ones (CA3c). CA1 and CA2 cells located in deep layers (towards stratum oriens) showed higher FRs than superficial ones (towards stratum radiatum). Higher FRs were notable during RUN for all regions except CA2, which fired more during WAKE. The lowest FRs were found during REM state.

The firing of the differently located neurons also varied during theta. CA1 pyramidal neurons fired in the ascending phase and CA3 pyramidal neurons on the descending phase. Although the preferred firing phase of CA1 cells remained constant from proximal to distal sites, a 180° shift was notable for deep cells during REM. Most of the neurons were highly modulated by theta, especially during REM compared to RUN state and in CA3 region compare to CA2 and CA1.

The connectivity between cells from distinct regions was different; while pyramidal cells from CA3a preferentially connect with the interneurons of proximal CA1, CA3c cells project more to distal CA1. From the CA2 region, more connected pairs were found with proximal CA1, especially from the CA2 deep cells toward the deep proximal CA1 interneurons. Also, more connections were found from CA2 toward CA3a compared with the CA3b and CA3c. The strength of the connectivity from CA3 to CA1 was stronger than the connectivity between CA2 and CA1.

Spatial coding properties along the hippocampal transverse axis

We found a larger number of place cells in CA2 and CA1 compared to CA3. Place cells with several fields were preferentially located in CA2, CA3a and distal CA1, whereas cells with one single field were found to

be in CA1 proximal and CA3c. The sizes of the fields were larger in CA1 distal sites compared to proximal CA1 and larger in CA3a compared to the CA3c border. In the CA1 and CA2 regions the FRs inside the fields of the deep cells were higher than their superficial peers. However, the FRs of the CA3 superficial cells were higher than the deeply located ones. The selectivity of the place cells was higher in CA3, increasing from CA3a to CA3c. In the CA1 region, proximal cells were more selective than distal ones and superficial cells showed higher selectivity compared to the deep ones. The CA3 neurons were more spatially informative than CA1, which also were more informative than CA2 cells. CA1 proximal cells had higher spatial information index than CA1 distal whereas these values increased from CA2 toward CA3c.

Phase precession showed different features between regions. We found that the phase range, which characterize the precession of the cells inside the theta cycle was shorter in CA2 and CA3 compare to CA1. Also, the slope and strength of the phase-position correlation was very sharp in CA1 whereas in CA2 and CA3 was smoother. Inside the CA1 region, the proximal CA1 cells showed higher strength than the distal cells.

Activation dynamics of hippocampal subregions during SPW-Rs

To study the contribution of different regions to SPW-Rs we examined the firing of the different populations of neurons and LFP patterns from the different regions during SPW-Rs. We found that ripples in CA2 generate two types of patterns: one with the classical response in CA1 (negative sharp-wave in stratum radiatum and positivity in the pyramidal

layer) and other with a negative wave in the stratum oriens and a positive wave in radiatum. The maximum power of the spectrograms during SPW-Rs detected in CA1 showed an earlier timing in the CA2 region in both SLEEP and WAKE states. In CA1 and CA3 the power was higher during SLEEP, whereas in CA2 the power was higher during WAKE.

We found that during SPW-Rs the firing dynamics of most of the neurons in CA1 and in all subregions of CA3 are positively modulated (increase their FR) both during ripples detected in CA1 and during ripples detected in CA2. In contrast, in the CA2 region only around half of the population was positively modulated during ripples detected in CA1, while the other half showed a slow ramp-like increase hundreds of milliseconds before the CA1 ripples, and became silent when the ripple occurs. Moreover, both of these populations uniformly increased their FR during CA2 ripples. We termed these groups as ripple-ramping cells (increasing the FR during CA2 ripples and silent during CA1) and phasic cells (increasing the FR during CA2 and CA1 ripples). The peak FR during ripples of the different subpopulations showed a temporal correlation with anatomy (CA2 ramping group is active first, then CA2 phasic, CA3a, CA3b, CA3c and finally CA1). The two subpopulations of CA2 showed an anatomical segregation, with ramping cells preferentially located in deep layers and phasic cells located in superficial layers.

Discussion

Connectivity, firing patterns and physiological properties of HP regions

The FRs of the neurons in the HP showed differences during behavioral states. The higher FR of all regions (except CA2) during RUN and the lower FR during REM are in line with the proposed theory suggesting that neuron's FRs are homeostatically regulated, increasing during waking due to sensory demands and decreasing during sleep. The higher FRs of CA2 during WAKE state account for the functional network located in CA2, which codes for positions during immobility.

Our functional monosynaptic analysis corroborated previous anatomical studies, showing the preference of CA3a subregion projections to the proximal CA1, CA3c to distal CA1, and the direct functional connections between CA2 and CA1. The higher strength of the connectivity between CA3 to CA1 could be related to the main pathway of information flow (through the trisynaptic pathway which last step goes from CA3 to CA1).

Theta phase locking and phase precession within the HP

We presented a comprehensive framework that integrates the theta phase preferences from the subregions of CA1 and CA3, as well as from the different pyramidal layer depths simultaneously. The gradual shift from the CA3c cells (descending phase) toward CA3a and CA2 cells (ascending phase, similar to CA1) could be due to the topology of the mossy fibers distribution along the CA3 axis (with a majority of fibers innervating CA3c and a lower number reaching CA3a and CA2). The

shift of the deep CA1 pyramidal cells during REM could account for the higher input from EC to these cells compared to their superficial peers. In the case of interneurons, the bimodal distribution of the preferred phase has been shown to be related with different subtypes of interneurons. Since these subtypes contribute to different network mechanisms, they become active during different parts of the theta cycle.

Phase precession characteristics were very different for the distinct regions. We hypothesized that this may be due to the different anatomical inputs from EC to the phase precessing cells at CA1, CA2, and CA3 areas. The higher strength of the phase-position correlation in proximal CA1 may be shaped by these differences. The different phase precession ranges of CA1 compared to CA2 and CA3 cells could be influenced by the combinations of inputs to these regions from different EC layers.

Spatial coding properties of different hippocampal subpopulations

The higher spatial selectivity of the CA3 cells match with the role of this region for pattern completion, operating as an autoassociative network, which allows for the association of a space with "rewards" and provides “completion” when demanded. The higher number of place fields per cell in distal CA1 and the single place fields of proximal CA1 cells were initially attributed to the differential projections of MEC to proximal CA1 and LEC axons to distal CA1. However, our finding in the CA3 axis (more place fields in CA3a compare to CA3c) suggest that CA3a could provide multi-field information to proximal CA1 and hence,

contribute to the specificity of this region compared to the lower specificity of distal CA1.

Mechanisms of SPW-Rs generation and propagation

Although originally it was proposed that SPW-Rs are generated in the CA3a region, where strong recurrent collaterals are present, the role of the CA2 region was never studied. We described two physiologically different subpopulations regarding their behavior during SPW-Rs (phasic and ramping cells respectively), and found that a propagation in time correlate with anatomy, being the CA2 region the initial excitable region when a SPW-R event is about to be detected. Population activity showed propagation from CA2 ramping cells, CA2 phasic, CA3a, CA3b, CA3c, and finally CA1. The CA2 cells mirror many aspects from the CA3a peers, including strong recurrent collaterals and high excitability properties, which could account for the ability of this region to trigger SPW-Rs. The two different LFP patterns that we found in CA2 correlate with a propagation from CA2-CA3-CA1 during SLEEP and a direct CA2-CA1 transmission during WAKE. This is not surprising since different behavioral states entrain different networks and more importantly, corroborate the special role of CA2 during immobility. Although there are several proposed theories, it is assumed that the underlying mechanisms of sharp-wave-ripple events are based on reaching a certain level of excitation, which triggers a population discharge. This can originate from the recurrent system of CA2-CA3a by several mechanisms (e.g. artificially triggered by external stimulation, by EC inputs or by single cells with adequate recurrent connectivity).

Acknowledgement

I thank Dr. Antal Berényi for giving me the opportunity to join his lab, for providing guidance and support. I thank Professor Gábor Jancsó and Professor Gyula Sáry for accepting me in the PhD Program and everyone else in the Department of Physiology for welcoming me. I thank Antonio, Misi, Gábor, Ancsa, Bereniké, Árpi, Yuichi and Mari, for helping me during my time in the lab. I thank Gergő Nagy for helping with experiments, Dr. Péter Hegyi and Dr. József Maléth, for providing access to the confocal microscope and Anett Nagy (and Anna), for helping with translations. I thank Professor György Buzsáki, for the scientific discussions and support. I thank everyone from the Biophysics Department of the Complutense University and from the Cajal Institute in Spain. I thank my family and Antonio, for being continuously supportive and help with everything I needed.

*Cover image was modified after the original drawing of Santiago Ramón y Cajal (in: Santiago Ramón y Cajal (1911) Histologie du Système nerveux de l'Homme et des Vertébrés, Paris: A. Maloine)

Publications related to the subject of the thesis

I. Oliva A, Fernandez-Ruiz A, Buzsaki G, Berenyi A (2016) Role of hippocampal region in triggering sharp-wave ripples. Neuron, in press. DOI: 10.1016/j.neuron.2016.08.008

II. Oliva A, Fernandez-Ruiz A, Buzsaki G, Berenyi A (2016) Spatial coding and physiological properties of hippocampal neurons in the Cornu Ammonis subregions. Hippocampus, in press. DOI: 10.1002/hipo.22659

III. Oliva A, Fernandez-Ruiz A (2016) Incorporating single cell contribution into network models of ripple generation. Journal of Physiology, in press. DOI: 10.1113/JP273062

Other publications

IV. Fernandez-Ruiz A, Oliva A (2016) Distributed representation of "what" and "where" information in the parahippocampal region. Journal of Neuroscience. 36(32):8286-8288.

Cumulative impact factor of the publications related to the thesis:

22.779 (ISI2015)

Cumulative impact factor of all publications:

28.703 (ISI2015)